CELL CYCLE
2021, VOL. 20, NO. 15, 1500–1517
https://doi.org/10.1080/15384101.2021.1950386

Taylor & Francis
Taylor & Francis Group

RESEARCH PAPER

Triple deletion of *TP53, PCNT*, and *CEP215* promotes centriole amplification in the M phase

Gee In Jung and Kunsoo Rhee

Department of Biological Sciences, Seoul National University, Seoul, Korea

ABSTRACT

Supernumerary centrioles are frequently observed in diverse types of cancer cells. In this study, we investigated the mechanism underlying the generation of supernumerary centrioles during the M phase. We generated the *TP53;PCNT;CEP215* triple knockout (KO) cells and determined the configurations of the centriole during the cell cycle. The triple KO cells exhibited a precocious separation of centrioles and unscheduled centriole assembly in the M phase. Supernumerary centrioles in the triple KO cells were present throughout the cell cycle; however, among all the centrioles, only two maintained an intact composition, including CEP135, CEP192, CEP295 and CEP152. Intact centrioles were formed during the S phase and the rest of the centrioles may be generated during the M phase. M-phase-assembled centrioles lacked the ability to organize microtubules in the interphase; however, a fraction of them may acquire pericentriolar material to organize microtubules during the M phase. Taken together, our work reveals the heterogeneity of the supernumerary centrioles in the triple KO cells.

ARTICLE HISTORY
Received 28 January 2021
Revised 6 June 2021
Accepted 28 June 2021

KEYWORDS
Centrosome; supernumerary centrioles; cell cycle; mitosis; CEP215; PCNT

Introduction

The centrosome is a subcellular organelle that functions as a major microtubule-organizing center in animal cells. The centrosome comprises a pair of centrioles surrounded by pericentriolar material (PCM). Duplication and separation of centrioles are closely linked to the cell cycle. When a cell enters the S phase, the daughter centrioles start assembling at a perpendicular angle to the mother centrioles and undergo elongation. Upon entering mitosis, the daughter centrioles disengage from the mother centrioles and remain associated until the end of mitosis [1–3]. Centriole separation is initiated at anaphase when separase cleaves pericentrin (PCNT), a major PCM protein [4,5]. Cleavage of PCNT induces disintegration of the mitotic PCM, resulting in the release of daughter centrioles from the mother centrioles at the mitotic exit [6].

When a cell exits the M phase, the daughter centriole becomes a young mother centriole. Daughter-to-mother centriole conversion is a process by which a centriole acquires PCM for performing the microtubule organization activity [7]. In addition, a young mother centriole functions as a template for the assembly of a new daughter centriole in the subsequent S phase [7]. One of the important events in this conversion may be the accumulation of CEP152, an adaptor of PLK4, in the young mother centriole [7,8]. CEP135, CEP295, and CEP152 accumulate sequentially into the daughter centrioles during the conversion [9,10].

PLK4 is a central regulator of centriole duplication and therefore, the levels and activity of PLK4 are tightly regulated during the cell cycle [11–13]. Centriole assembly cannot start at the G1 phase because PLK4 activity is maintained at a low level in this phase. Once PLK4 activity is induced near the S phase, the daughter centrioles assemble using the mother centrioles as templates. Upon binding to STIL, PLK4 is activated via trans-autophosphorylation and subsequently phosphorylates STIL, triggering the centriolar recruitment of SAS6 for cartwheel formation [14–18]. Mother centrioles are not allowed to form new daughter centrioles in the G2 and M phases, as long as they

CONTACT Kunsoo Rhee rheek@snu.ac.kr
Supplemental data for this article can be accessed here

are associated with daughter centrioles in their vicinity [19,20].

Supernumerary centrioles are frequently observed in diverse types of cancer cells [21,22]. Several mechanisms causing centriole amplification have been suggested, including centriole over-duplication, de novo centrosome formation, fragmentation of overly elongated centrioles, and cytokinesis failure [23]. Most importantly, overexpression of PLK4 generates multiple daughter centrioles during the S phase [13,24]. Genetic variants near the *PLK4* gene are closely associated with aneuploidy [25] and PLK4 overexpression has been reported in a variety of tumor cells [26]. Moreover, the involvement of PLK1 in centriole amplification has been reported. PLK1 is a novel regulator of centriole elongation in human cells [27] and prolonged activity of PLK1 leads to mitotic centriole over-elongation [28]. Over-elongated centrioles can also contribute to centrosome amplification via fragmentation or formation of multiple procentrioles along their elongated walls [22,29].

PCM is organized as a toroid around mature centrioles in the interphase and expands into an amorphous structure during mitosis [30–32]. PCNT and CEP215, two major PCM proteins in the human centrosome [33–36], specifically interact with each other in both interphase and mitosis and act as scaffolds for the γ-tubulin ring complex [37]. Previous reports have suggested that *CEP215* mutations cause autosomal recessive primary microcephaly [38]. Likewise, *PCNT* mutations were reported to cause microcephalic osteodysplastic primordial dwarfism, as well as other diseases, such as cancers and mental disorders [39,40].

In the present study, we investigated the role of PCM in centriole configuration during mitosis. When the cells were treated with mitotic drugs, such as S-trityl-L-cysteine (STLC) and nocodazole, for an extended period, the centrioles are liberated from the PCM [1,3]. Based on these observations, we previously proposed that PCM might be important for centriole association within the centrosome during mitosis [3]. We also reported that centrioles prematurely separate and eventually amplify when *PCNT* is deleted and interpreted that the absence of PCNT generates defects in mitotic PCM, which holds the mother and daughter centrioles together [41]. In this study, we generated the *TP53, PCNT*, and *CEP215* triple knockout (KO) cells and determined the centriole configurations during mitosis. We also followed the fate of supernumerary centrioles in these triple KO cells.

Results

Deletion of CEP215 leads to premature centriole separation during mitosis

To investigate the role of CEP215 in centriole engagement, we generated *CEP215*-deletion cells using the CRISPR/Cas9 method. *CEP215* was deleted in the *TP53* knockout HeLa cells, because the p53-dependent checkpoint pathway is frequently activated in cells devoid of centrosome proteins [42,43]. The absence of CEP215 was confirmed by immunoblotting and immunostaining analyses (Supplemental Figure S1). We determined centriole configurations during mitosis in the *CEP215*-deleted HeLa cells. The cells were arrested at prometaphase with STLC, an Eg5 inhibitor, and coimmunostained with centrin2 (CETN2) and CEP135 antibodies. The control cells revealed two centriole pairs with a 2:1 ratio of CETN2 and CEP135, indicating centriole engagement [4,41] (Figure 1(a–c)). As previously reported, 85% of the *PCNT*-deleted cells had a 1:1 ratio of CETN2 and CEP135, indicating that the mother and daughter centrioles were precociously separated at the M phase [41] (Figure 1(a–c)). About half of the centriole pairs in the *CEP215*-deleted cells disengaged but remained within the same centrosome, suggesting that CEP215 is partly involved in centriole engagement [44,45] (Figure 1(a–c)).

We rescued *CEP215*-deleted cells with ectopic Flag-CEP215 to determine centriole configurations in M phase-arrested cells. As expected, centriole engagement was restored with Flag-CEP215, but not with Flag-CEP215$^{\Delta C}$ which lacks the CM2 domain for interaction with PCNT and other centrosome proteins [37,46] (Figure 1(d,e)). Centriole engagement was not restored with Flag-CEP215$^{\Delta C+PACT}$, whose centrosome localization was enforced with the PACT domain [47] (Figure 1(d,e)). This result suggests that CEP215 and PCNT cooperatively regulate the centriole configuration during mitosis.

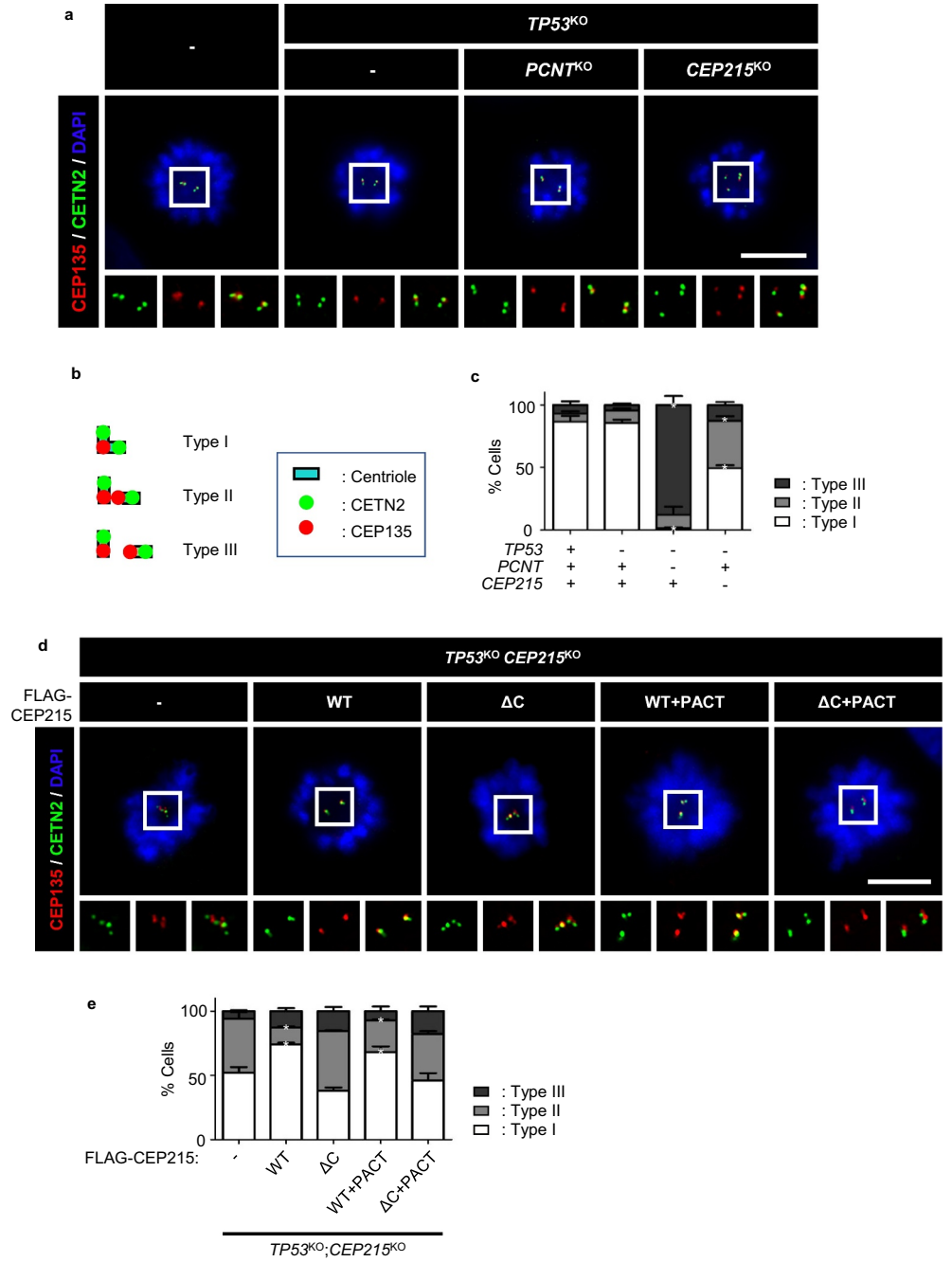

Figure 1. Precocious centriole separation in *CEP215*-deleted cells during mitosis (a) The *CEP215*- or *pericentrin* (*PCNT*)-deleted HeLa cells were arrested at prometaphase with STLC and subjected to coimmunostaining analysis with centrin-2 (CETN2; green) and CEP135 (red) antibodies. Scale bar, 10 μm. (b) Engaged centrioles were determined with 2:1 ratio of the CENT2 and CEP135 signals (Type I). Centriole separation was determined with 1:1 ratio (Type III). Type II indicates that the centrioles separated but remained within the same centrosome. (c) The number of cells with three types of centrioles were counted. (d) The *CEP215*-deleted cells were stably rescued with ectopic FLAG-CEP215 (WT, ΔC, WT + PACT and ΔC + PACT). The cells were arrested at prometaphase and subjected to coimmunostaining analysis with the CETN2 (green) and CEP135 (red) antibodies. Scale bar, 10 μm. (e) The number of cells with three types of centrioles were counted. (c, e) Greater than 30 cells per group were analyzed in three independent experiments. Values are means and SEM. The statistical significance was analyzed using t-test compared to the control within the same group (*, $P < 0.05$).

Generation of the TP53;PCNT;CEP215 triple knockout cell lines

To determine the cooperative functions of CEP215 and PCNT in centriole configurations during mitosis, we generated *TP53, PCNT*, and *CEP215* triple KO cells. During the selection step, we realized that the triple KO cells failed to form a stable cell line due to low proliferation activity and cell death (data not shown). Therefore, triple KO cells were generated in the presence of the ectopic PCNT gene with a destabilization domain (*DD-PCNT*), whose expression can be induced by doxycycline and shield1 [41]. Immunoblot analysis revealed that PCNT and CEP215 levels were below the detection limit in the triple KO cells (Figure 2(a)). Immunostaining analysis also confirmed that the PCNT and CEP215 signals were absent in the centrosomes of the triple KO cells (Figure 2(b–d)). These results indicated that *TP53, PCNT*, and *CEP215* triple KO cell lines were properly generated.

Precocious centriole separation and amplification in the triple KO cells during the M phase

We examined the precocious separation and amplification of centrioles in the M phase in *TP53, PCNT*, and *CEP215* triple KO cells. The cells were arrested at prometaphase using STLC, and centriole engagement was determined (Figure 3(a)). The absence of PCNT and CEP215 was confirmed by immunoblot analysis (Figure 3 (b)). Precocious centriole separation and supernumerary centrioles were observed in approximately 85% and 30% of the *PCNT*-deleted cells, respectively (Figure 3(c–e)). Precocious centriole separation was observed in about half of the *CEP215*-deleted cells, but supernumerary centrioles were not detected in these cells (Figure 3(c,d)). In the case of the triple KO cells, precocious centriole separation was evident and centriole amplification was fortified in up to 70% of them (Figure 3(c–e)). Indeed, some of the triple KO cells included up to 30 extra centrioles (data not shown). These results reveal a cooperative function of PCNT and CEP215 in the prevention of precocious centriole separation and amplification during mitosis.

The knockout phenotypes were also determined in cells during the M phase without a mitotic drug (Figure 3(f)). Precocious separation of centrioles was detected in most of the naturally dividing triple KO cells (Figure 3(g,h)). Supernumerary centrioles were also detected, although, the incidence was reduced to 40% (Figure 3(g,i)). It is likely that the triple KO phenotypes are stronger in the M phase-arrested cells than in the naturally dividing cells. Nonetheless, it is evident that precocious centriole separation and amplification do not result from the mitotic drug treatment but from the absence of CEP215 and PCNT.

Supernumerary centrioles in the triple KO cells during the cell cycle

To investigate the fate of supernumerary centrioles in triple KO cells, we traced the centrioles throughout the cell cycle. Since the PLK4-overexpressing cells also generate extra centrioles, they were used as a control [13,48]. Supernumerary centrioles were generated by the induction of PLK4 overexpression using doxycycline (Figure 4(a)). The M-phase populations of the PLK4-overexpressing cells and the triple KO cells were collected using the mitotic shake-off method. The cells synchronously entered the G1 phase and were cultured for the indicated time periods of up to 24 h (Figure 4(a)). In control cells, two centrioles were observed after 2 h of mitotic shake-off, which increased to four after 17 h when most of the cells entered the S phase (Figure 4(c)). The centriole number eventually reduced to two after 24 h of completion of the next mitotic cycle (Figure 4(b,c)). The PLK4-overexpressing cells included extra centrioles at the beginning of the culture, and 60% of them had five or more centrioles at 17 h, indicating that daughter centrioles were newly assembled during the S phase (Figure 4(b,c)). The triple KO cells also included multiple centrioles in the G1 phase (Figure 4(b,c)). However, unlike the PLK4-overexpressing group, the number of centrioles in the triple KO cells only slightly increased during the S phase (Figure 4(b,c)). These results suggest that supernumerary centrioles in the triple KO cells might survive, but do not duplicate during the interphase.

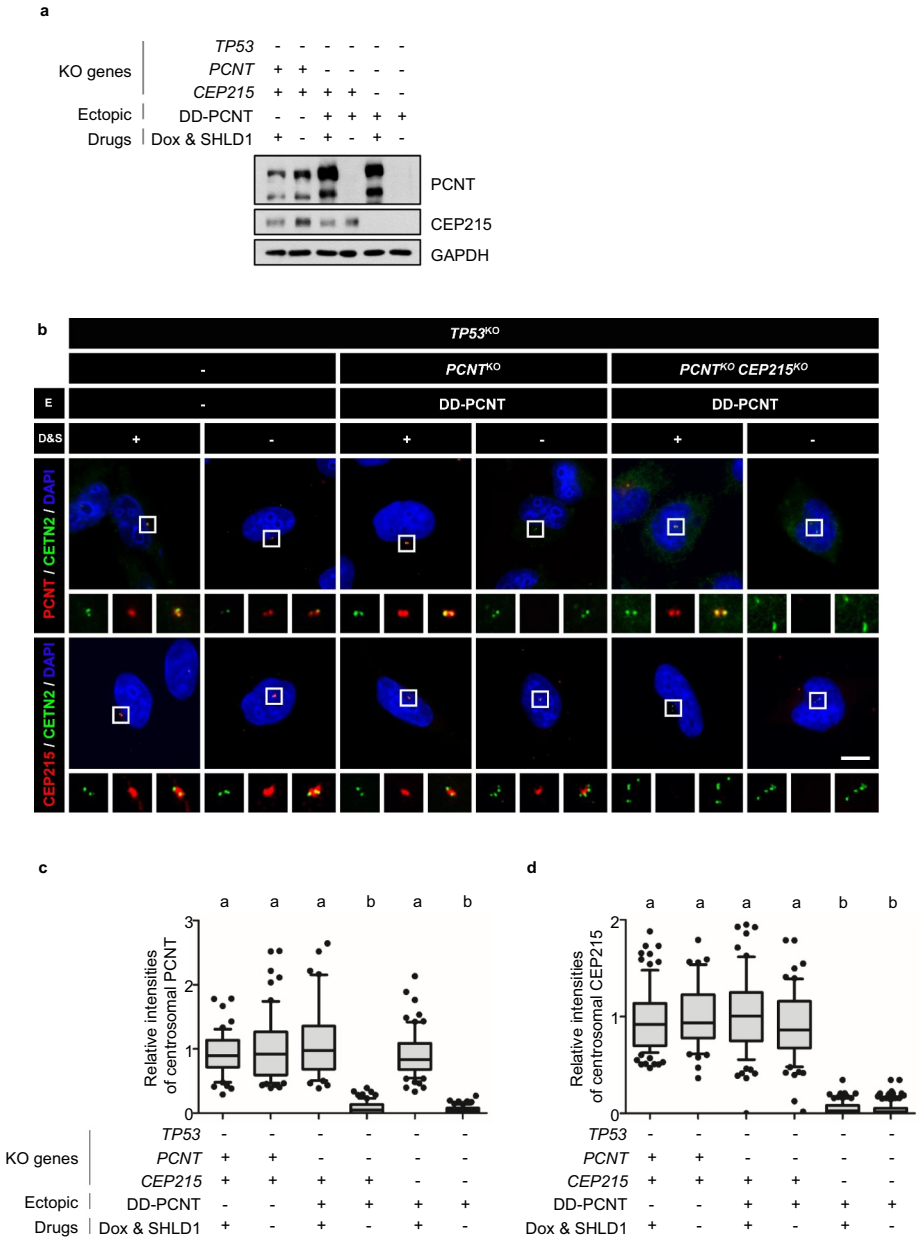

Figure 2. Generation of the *TP53;PCNT;CEP215*-deleted cells (a) The *TP53, PCNT*, and *CEP215* genes were deleted in HeLa cells using the CRISPR/Cas9 method. Endogenous *PCNT* was deleted in the presence of the ectopic *DD-PCNT* gene whose expression is induced by doxycycline (Dox) and shield1 (SHLD1). The deletions were confirmed via immunoblotting analysis with antibodies specific to PCNT, CEP215, and GAPDH. (b) The KO cells were coimmunostained with antibodies specific to CETN2 (green), PCNT (red), and CEP215 (red). Nuclei were stained with DAPI (blue). Scale bar, 10 μm. (c, d) Relative intensities of the centrosomal PCNT (c) and CEP215 (d) signals were determined. Greater than 30 cells per group were analyzed in three independent experiments. Relative intensities of the centrosome signals are presented with the box and whisker plots. The statistical significance was analyzed using one-way ANOVA and indicated using lower case alphabets ($P < 0.05$).

To determine the PLK4-dependent centriole assembly in the triple KO cells during S phase, we used centrinone, a PLK4 inhibitor [49]. As expected, centriole assembly was significantly reduced in the control and PLK4-overexpressing cells during the S phase (Figure 4(d)). In contrast, centrinone had little effect on the centriole assembly in the triple KO cells, confirming that centriole assembly in the triple KO cells was very limited during the S phase (Figure 4(d)).

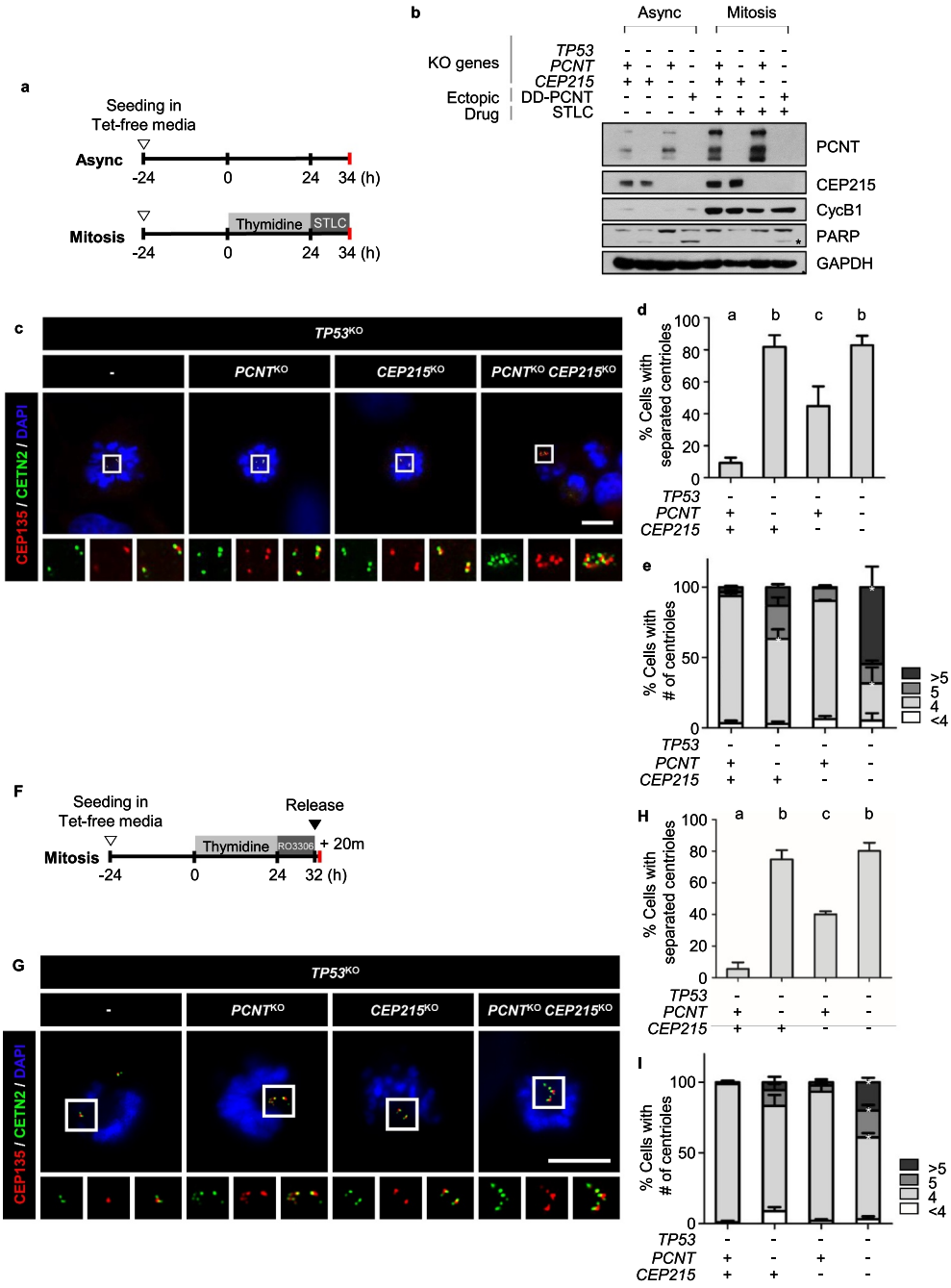

Figure 3. Precocious centriole separation and amplification of the triple KO cells during M phase (a) Timeline for preparation of prometaphase cells. The KO cells were treated with thymidine for 24 h followed by STLC for 10 h. (b) Immunoblot analyses were performed with antibodies specific to PCNT, CEP215, cyclin B1, and GAPDH. (c) The cells were subjected to coimmunostaining analysis with the CETN2 (green) and CEP135 (red) antibodies. Nuclei were stained with DAPI (blue). Scale bar, 10 μm. (d) The number of cells with separated centrioles were counted. (e) The number of centrioles per cell were counted. (f) Timeline for the preparation of naturally dividing prometaphase cells. The triple KO cells were treated with thymidine for 24 h, followed by RO3306 for 8 h, and released for 20 min. (g) The cells were subjected to coimmunostaining analysis with the CETN2 (green) and CEP135 (red) antibodies. Nuclei were stained with DAPI (blue). Scale bar, 10 μm. (h) the number of cells with separated centrioles were counted. (i) The number of centrioles per cell were counted (D, E, H, I). Greater than 30 cells per group were analyzed in three independent experiments. Values are means and SEM. The statistical significance was analyzed using one-way ANOVA (d, h) and t-test compared to the control within the same group (e, i). ($P < 0.05$).

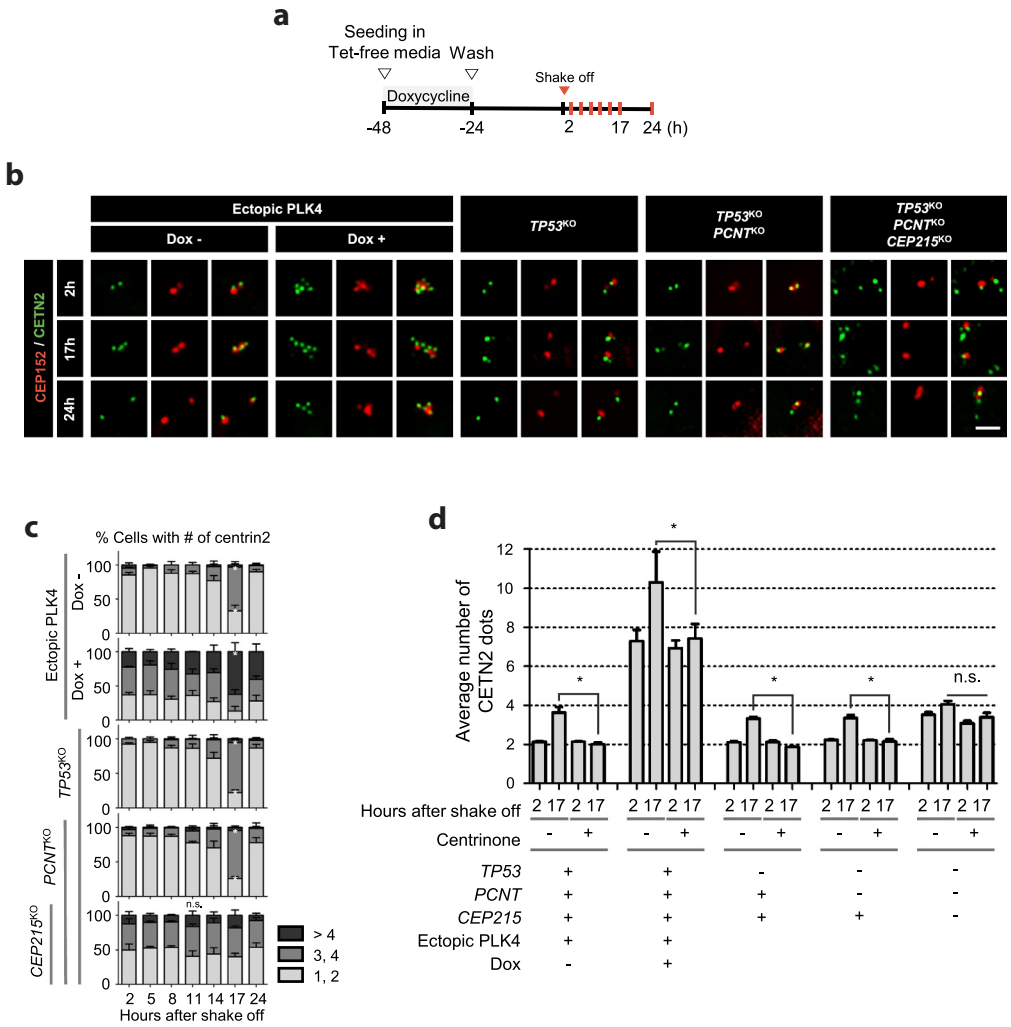

Figure 4. Centriole numbers throughout the cell cycle in the triple KO cells (a) Timeline for preparation of synchronous interphase cells. Cells were treated with doxycycline for 24 h to induce ectopic PLK4 expression, washed out and cultured for another 24 h. After the mitotic shake-off, the cells were cultured for up to 24 h. (b) The PLK4-overexpressing and KO cells were subjected to coimmunostaining analysis with the CETN2 (green) and CEP152 (red) antibodies. Scale bar, 2 μm. (c) The number of CETN2 dots were counted at indicated time points. (d) After the mitotic shake-off, the PLK4-overexpressing and KO cells were cultured in the presence of centrinone for 2 h and 17 h, and immunostained with the CETN2 antibody. The number of CETN2 dots per cell were counted. (c, d) Greater than 30 cells per group were analyzed in three independent experiments. Values are means and SEM. The statistical significance was analyzed using t-test between the indicated groups (n.s., not significant; *, $P < 0.05$).

Nascent centriole formation in the triple KO cells during mitosis

To determine the unscheduled centriole assembly during mitosis, we used cells transfected with the *CETN2-Dendra2* plasmid. Dendra2 is a photoconvertible fluorescent protein that can be activated by ultraviolet light [50]. Photoactivation induces the red fluorescent signals in addition to the green fluorescent signals in the centrioles with CETN2-Dendra2 [50]. When the CETN2-Dendra2-expressing, control cells were photoactivated during the M phase, two pairs of centrioles were marked with both green and red fluorescence (Figure 5(a)). The triple KO cells had multiple centrioles with both red and green fluorescence, but also included centrioles with green-only fluorescence (Figure 5(a)). Therefore, we recorded live images of CETN2-Dendra2-expressing cells to determine the M-phase assembly of centrioles in the triple KO cells. Toward this goal, we arrested the CETN2-Dendra2-expressing cells at G2 phase with RO3306 and photoactivated them (Figure 5(b)). After the cells were liberated

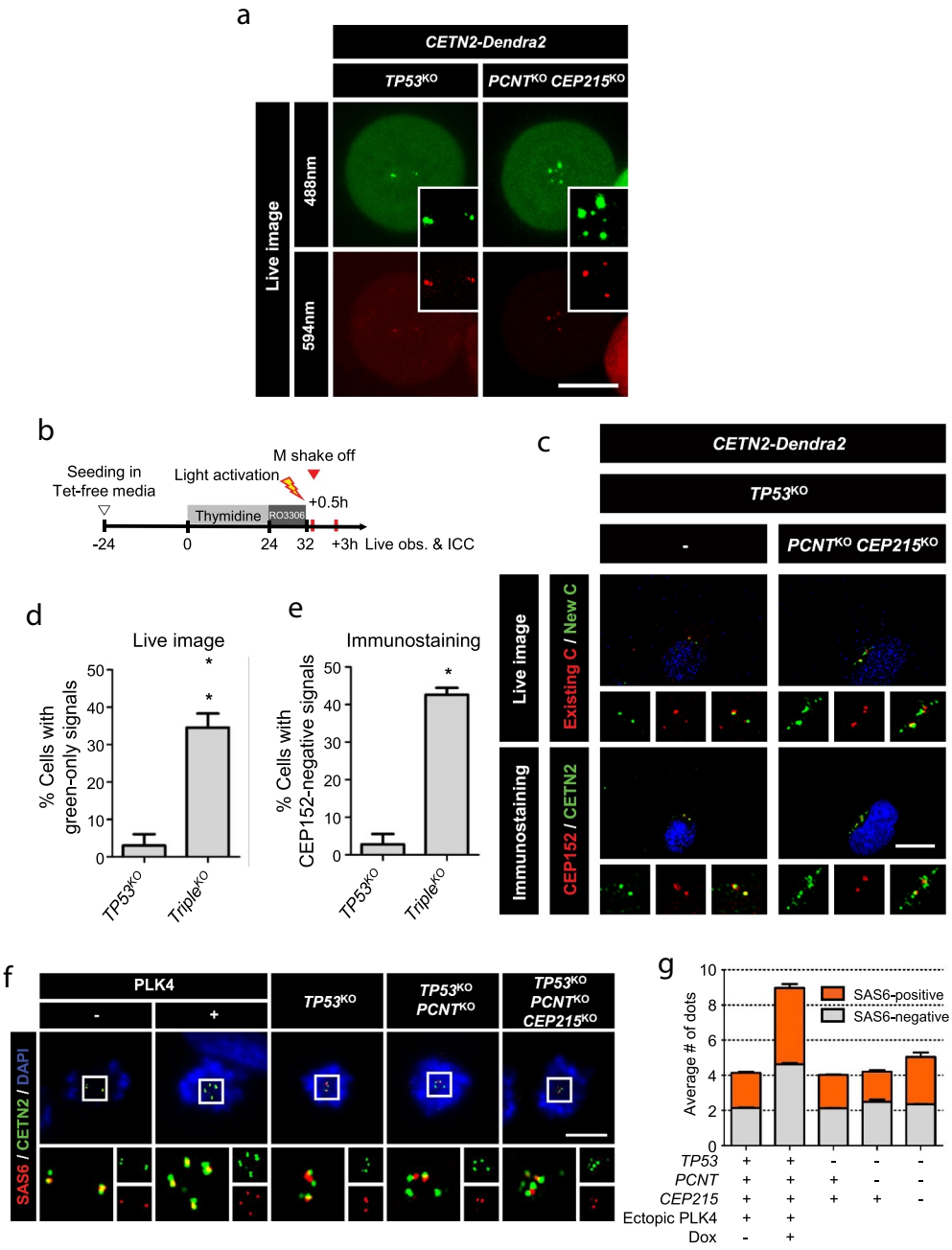

Figure 5. Centriole assembly during M phase in the triple KO cells (a) CETN2-Dendra2 was stably expressed in the triple KO cells. The cells were treated with thymidine for 24 h followed by STLC for 7 h, and light-activated. The CETN2-Dendra2 signals were observed for up to 2 h after the activation. Light activation makes CETN2-Dendra2 detected with both 448 and 594 nm fluorescent light (green and red). Scale bar, 4.42 μm. (b) The triple KO cells stably expressing CETN2-Dendra2 were treated with thymidine for 24 h, followed by RO3306 for 8 h, and light-activated. Thirty minutes after the release, mitotic cells were collected by the shake-off method, and cultured for 3 h. (c) We recorded the fluorescent signals of the cells, and fixed them for coimmunostaining analysis with antibodies specific to CETN2 and CEP152. Scale bar, 10 μm. (d) The number of cells with green-only centrioles were counted. (e) The number of cells with CEP152-negative centrioles were counted. (d, e) Greater than 20 cells per group were analyzed in three independent experiments. The statistical significance was analyzed using t-test (* $P < 0.05$). (f) The PLK4-overexpressing and KO cells were treated with STLC for 10 h and subjected to coimmunostaining analysis with the CETN2 (green) and SAS6 (red) antibodies. Scale bar, 10 μm. (g) The number of SAS6-positive (orange) and -negative (gray) CETN2 dots were counted. Greater than 30 cells per group were analyzed in three independent experiments. Values are means and SEM.

from the G2 arrest, passed the M phase, and reached the G1 phase, they were recorded for the fluorescent signals and subsequently fixed for coimmunostaining analysis (Figure 5(b)). We observed that the control cells included a pair of centrioles with both green and red fluorescent signals (Figure 5(c)) The centriole pairs were also coimmunostained with the CETN2 and CEP152 antibodies, indicating that they are mother centrioles which had been assembled during the previous S phase (Figure 5(c)). In the case of the triple KO cells, multiple centrioles were observed in approximately 35% of the cells, and they included green-only fluorescent centrioles (Figure 5(c,d)). Some of the multiple centrioles in the triple KO cells were not immunostained with the CEP152 antibody (Figure 5(c,e)). These results support the notion that, in triple KO cells, unscheduled centriole assembly occurs in the M phase.

SAS6 is present only in the daughter centrioles immediately after assembly and disappears during mitosis. Since the SAS6 signal is absent in the mother centriole, it can be used as an indicator to distinguish daughter centrioles from the mother centrioles [49]. Prometaphase-arrested cells were coimmunostained with SAS6 and CETN2 antibodies (Figure 5(f)). As expected, there were two SAS6-negative signals in the control cells, indicating the presence of two mother centrioles. In the case of the PLK4-overexpressing cells, more than four SAS6-negative signals were detected, indicating the presence of multiple mother centrioles in mitotic cells (Figure 5(g)). The same number of SAS6-positive signals were also detected, suggesting that multiple daughter centrioles were generated from approximately the same number of mother centrioles (Figure 5(g)). In the case of the triple KO cells, approximately two SAS6-negative centrioles were detected, indicating that there were two mother centrioles (Figure 5(g)). However, the number of SAS6-positive signals exceeded that of SAS6-negative centrioles (Figure 5(g)) indicating that one or more daughter centrioles may be formed from a single mother centriole in the triple KO cells. Furthermore, nascent daughter centrioles in the triple KO cells may be assembled in a SAS6-dependent manner during mitosis.

Mother-to-daughter centriole conversion in the precociously amplified centrioles

We determined the intactness of supernumerary centrioles in triple KO cells. CEP152 is a mother centriole protein that functions as an adaptor for PLK4 [51]. In control cells, there were two CEP152-positive centrioles throughout the cell cycle (Figure 6(a)). In contrast, approximately 40% of the PLK4-overexpressing cells included three or more CEP152-positive centrioles at the beginning of the culture, and this proportion was maintained throughout the cell cycle (Figure 6(a)). This observation is consistent with a previous report that PLK4-overexpressing cells include multiple mother centrioles [48]. Interestingly, the triple KO cells had only two CEP152-positive centrioles out of multiple centrioles, and this number was maintained throughout the cell cycle (Figure 6(a)). These results suggest that, in the triple KO cells, only a single daughter centriole converts to a mother centriole during mitotic exit. These results also indicate that only a pair of centrioles may exclusively recruit PLK4 to generate new daughter centrioles during the S phase.

To examine the intactness of the centrioles in the triple KO cells, we performed coimmunostaining analyses with CEP152 and CETN2, along with selected centrosome proteins in the early G1 phase (Figure 6(b)). As expected, most of the centrioles in the control cells were CEP152-positive and coimmunostained with antibodies specific to CEP295, CEP192, CEP135, and γ-tubulin (Figure 6(b)). Likewise, over 90% of the multiple centrioles in the PLK4-overexpressing cells coimmunostained with all the antibodies mentioned above (Figure 6(b)). However, only two centrioles in the triple KO cells were positive for CEP152 (Figure 6(b)). Furthermore, CEP295, CEP192, CEP135, and γ-tubulin were detected almost exclusively in the CEP152-positive centrioles (Figure 6(b)). These results strongly suggest that only a pair of CEP152-positive centrioles were intact mother centrioles in the triple KO cells, whereas the others were defective centrioles.

Since CEP152 is an adapter protein for PLK4, its recruitment is considered as a critical event for daughter-to-mother centriole conversion [10,51,52]. Centriolar localization of CEP295

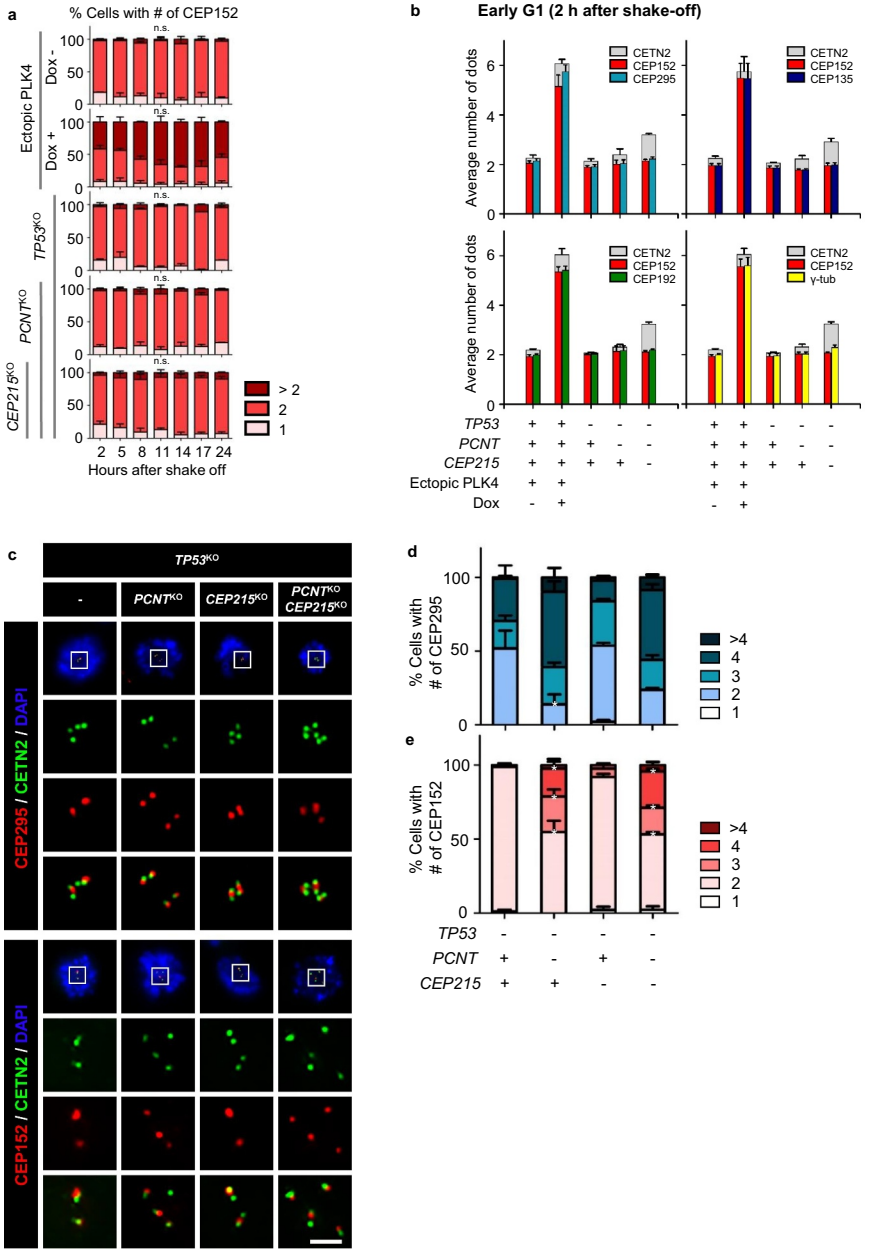

Figure 6. Intactness of the centrioles in the triple KO cells (a) Mitotic cells were collected with the mitotic shake-off method and cultured for up to 24 h. The number of CEP152 dots was counted at indicated time points. The statistical significance was analyzed using the t-test compared to the 2 h values within the same groups (n.s., not significant; * $P < 0.05$). (b) The G1 phase cells were coimmunostained with antibodies specific to CEP295, CEP192, CEP135 and γ-tubulin, along with CETN2 and CEP152. The number of centrioles with CEP152 and the indicated protein signals were counted. (c) The cells were arrested at prometaphase and subjected to coimmunostaining analysis with the CETN2 (green) and CEP295 or CEP152 (red) antibodies. Scale bar, 2 μm. (d, e) The numbers of CEP295 and CEP152 signals were counted in the cells. The statistical significance was analyzed using t-test compared to the control within the same group (* $P < 0.05$). (A, B, D, E) Greater than 30 cells per group were analyzed in three independent experiments. Values are means and SEM.

precedes that of CEP152 [9,10,53]. To determine when the daughter-to-mother centriole conversion occurs in the triple KO cells, we coimmunostained M-phase-arrested cells with the CEP295 and CEP152 antibodies (Figure 6(c)). The results showed that less than half of the control and *CEP215*-deleted cells included more than three CEP295 signals (Figure 6(c,d)), and a few of them contained more than three CEP152 signals (Figure 6(c,e)). Contrastingly, multiple CEP295 signals were detected in majority of the *PCNT*-deleted cells (Figure 6(c,d)). Multiple CEP152

signals were also detected in half of them (Figure 6(c,e)). These results suggested that daughter centrioles readily converted to mother centrioles even in the M phase, as soon as they departed from the mother centrioles.

Defective microtubule organization in the triple KO cells

To determine PCM accumulation in the supernumerary centrosomes, we coimmunostained the interphase and mitotic cells with CEP192 and γ-tubulin antibodies (Figure 7(a)). Consistent with the previous results, 95% of the control and KO cells had only two centrosomes positive for CEP192 and γ-tubulin in the interphase (Figure 7(a,b)). In mitotic control cells, both CEP192 and γ-tubulin signals were detected in two centrosomes (Figure 7(a,b)). However, both the CEP192 and γ-tubulin signals were also detected in many of the separated and amplified centrioles of the KO cells during mitosis (Figure 7(a,b)). This result suggests that precociously separated and amplified centrioles may occasionally have an ability to organize microtubules during mitosis.

We performed microtubule regrowth assays to determine the biological activities of the centrosomes in the PLK4-overexpressing and the triple KO cells. In control cells, microtubules started to become organized from both the centrosomes present in the G1 phase (Figure 7(c,d)). About six centrosomes were present in the PLK4-overexpressing cells, and 91% of them were able to organize microtubules (Figure 7(c,d)). However, in the tripled KO cells, only 73% of the centrosomes organized microtubules, leaving 27% of them without an activity (Figure 7(c,d)). These results suggest that a significant proportion of the centrosomes in the triple KO cells have functional defects in microtubule organization during interphase.

Next, we determined spindle configurations in mitotic cells of PLK4-overexpressing and triple KO cells. Spindle phenotypes were categorized into five groups: lagging chromosomes, chromosome misalignment, monopole, bipole, and multipole [54] (Figure 7(e)). As expected, approximately 80% of the mitotic control cells formed bipolar spindles (Figure 7(f)). In PLK4-overexpressing cells, approximately 60% of the mitotic cells formed multipoles (Figure 7(f)). In contrast, the proportion of monopoles significantly increased by up to 40% in the triple KO cells (Figure 7(f)). These results suggest that many of the separated centrioles in the triple KO cells have a limited ability to function as spindle poles during mitosis.

Discussion

We previously reported that the centriole pairs in *PCNT*-deleted cells were prematurely separated and occasionally amplified during mitosis [41]. In this study, we observed that centriole amplification was significantly fortified in mitotic cells lacking both *PCNT* and *CEP215*. These results strongly support the notion that PCM is essential for maintaining centriole pairs within mitotic centrosomes. Otherwise, the centrioles are liberated from the inhibitory environment and start to function as templates for centriole assembly during mitosis [1,3] (Figure 8).

It was previously suggested that CEP215 is required for proper centriole configuration within the centrosomes. Centrioles are detached from the spindle poles in *CEP215*-depleted mitotic cells [55,56]. The incidence of abnormal centriole configurations and occasional amplification has been reported in embryonic fibroblasts of *CEP215* mutant mice [44]. Consistent with previous reports, half of the centrioles disengaged in the *CEP215*-deleted cells, but they were still retained within the centrosomes. Centrioles in *CEP215*-deleted cells may not become templates for centriole assembly because of short-range inhibitory signals from each other [1]. However, centrioles are actively generated when both *CEP215* and *PCNT* are deleted simultaneously. It is likely that PCNT and CEP215 cooperatively constitute mitotic PCM for proper centriole configuration during the M phase. PCNT may be important for mitotic PCM formation, while CEP215 may be critical for the prevention of unscheduled centriole amplification in the M phase.

It is known that PLK4 activity increases in the S phase and remains high until the end of mitosis [57]. Nonetheless, centrioles in the triple KO cells were not amplified in the S and G2 phases (Figure 4(c,d)). We observed that the centriole

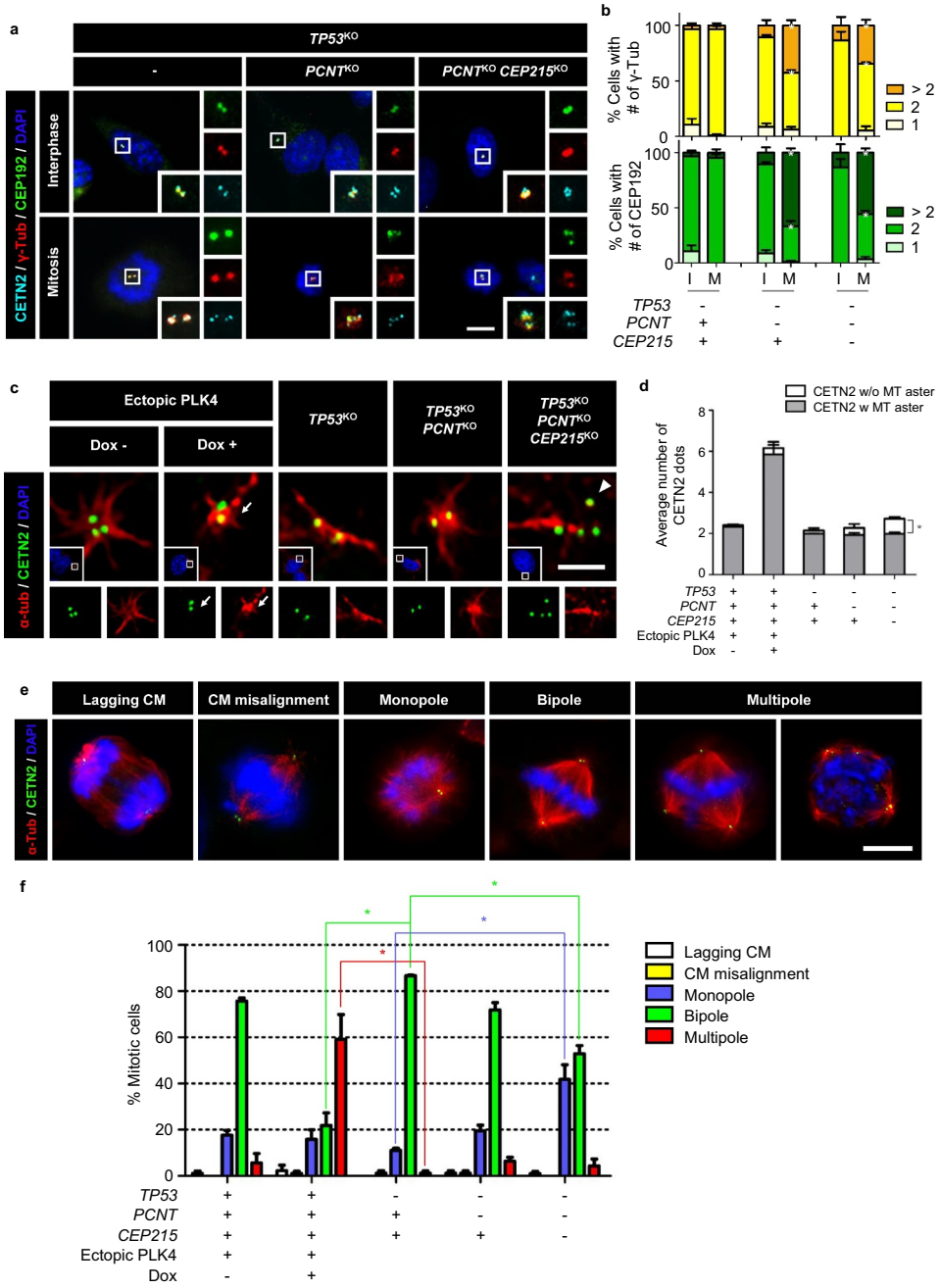

Figure 7. Spindle defects in the triple KO cells (a) The KO cells at interphase and mitosis were subjected to coimmunostaining analysis with antibodies specific to CEP192 (green), γ-tubulin (red) and CETN2 (cyan). Scale bar, 10 μm. (b) The number of CEP192 and γ-tubulin signals were counted in cells at interphase (i) and mitosis (m). (c) The PLK4-overexpressing and triple KO cells at G1 phase were subjected to microtubule regrowth assays. The cells were coimmunostained with antibodies specific to CETN2 (green) and α-tubulin (red). Scale bar, 2 μm. (d) The number of CETN2 dots with microtubule asters were counted. (e) The PLK4-overexpressing and KO cells at mitosis were subjected to coimmunostaining analysis with the CETN2 (green) and α-tubulin (red) antibodies. DNA was stained with DAPI (blue). Representative spindle abnormalities were shown. Scale bar, 10 μm. (f) Mitotic cells with abnormal spindles were counted. (B, D, F) Greater than 30 cells per group were analyzed in three independent experiments. Values are means and SEM. The statistical significance was analyzed using t-test (*, $P < 0.05$).

pairs in the G2 phase were surrounded by other PCM proteins, such as γ-tubulin and CEP192, even in the absence of CEP215 and PCNT (Supplemental Figure S2). These results reveal that the interphase PCM maintains an intact toroid structure even without PCNT and CEP215. Another possibility may be that the daughter centriole is physically linked to the mother centriole

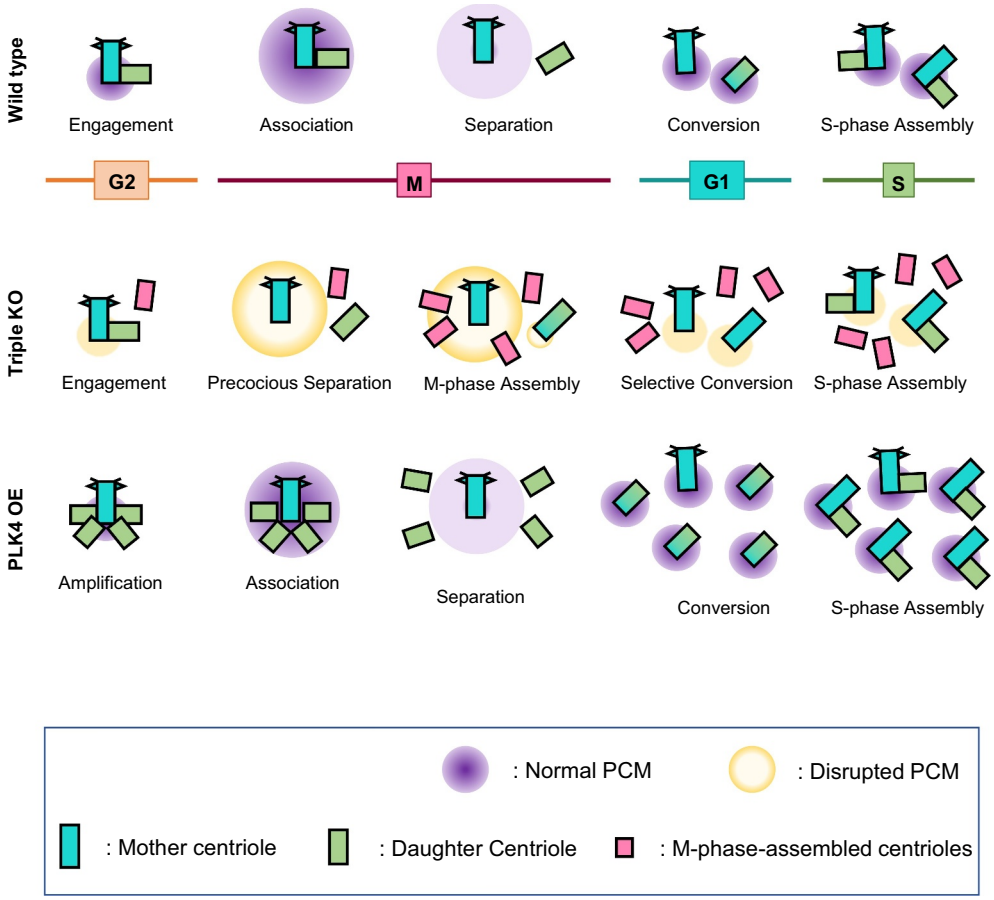

Figure 8. Model for the generation of supernumerary centrioles at M phase. After entering the M phase, the daughter centrioles readily disengage from mother centrioles, but remain associated within the same mitotic centrosomes. Daughter centrioles eventually separate from the mother centrioles after PCM is disintegrated at the end of mitosis. Simultaneous deletion of *PCNT* and *CEP215* makes mitotic PCM disorganized, resulting in the precocious separation of the centrioles at M phase. Since the centrioles are liberated from the inhibitory environment against centriole assembly, they start to function as templates for centriole assembly even in M phase. However, these M-phase-assembled centrioles may not organize microtubules, nor function as templates for centriole assembly in the subsequent S phase. In contrast, PLK4 overexpression generates supernumerary centrioles at S phase, most of which may function as templates for centriole assembly in the subsequent S phase.

even without PCM until the initiation of mitosis so that precocious centriole amplification does not occur.

When we traced the fate of the supernumerary centrioles during the cell cycle, we found that only two out of many centrioles maintained an intact composition in the triple KO cells (Figure 6). In contrast, most of the multiple centrioles were intact in the PLK4-overexpressing cells, which doubled during the subsequent S phase (Figure 4). It remains to be investigated why the triple KO cells included only two CEP152-positive centrioles in the interphase. We suspect that two CEP152-positive centrioles might have been generated in the previous S phase, while the other centrioles were assembled at the M phase. M phase centrioles may be formed following a general assembly process with the SAS6 cartwheel structure. However, centriole assembly may not be completed within the short duration of the M phase. The M-phase-assembled centrioles may be smaller than the S-phase-assembled centrioles, as evidenced by the observation that the newly made M phase centrioles had smaller CETN2 signals than the others in the live image analysis. As a result, M-phase-assembled centrioles may not contribute to the formation of spindle poles during mitosis. Furthermore, the M-phase-assembled centrioles may not be able to recruit a series of centrosome proteins necessary for daughter-to-

mother centriole conversion at the end of mitosis [7]. Triple KO cells often form monopolar spindles during mitosis, possibly due to the absence of a critical factor, such as CEP192, for bipolar spindle formation [58]. The factors that are critically absent in M-phase-assembled centrioles for spindle pole formation and mother-to-daughter centriole conversion remain to be identified.

Supernumerary centrioles are common in cancer cells [21,22]. Many cells with supernumerary centrioles may complete mitosis by forming a bipolar spindle with clustered centrosomes [59]. Nonetheless, bipolar spindle formation via centrosome clustering is associated with an increased frequency of lagging chromosomes during anaphase, thereby explaining the link between supernumerary centrosomes and chromosomal instability [59]. In this work, we report the heterogeneity of supernumerary centrioles in *TP53; PCNT;CEP215*-deleted cells. Although supernumerary centrioles were found in triple KO cells, only two of them appeared intact. The M-phase-assembled centrioles in the triple KO cells might not be as active as the S-phase-assembled centrioles. Nonetheless, they still have a chance to organize microtubules and disturb the spindle formation during mitosis. Future studies are needed to determine the heterogeneity of the centrioles in diverse cancer cells.

Materials and methods

Cell culture, generation of deleted cell lines, and synchronization

The deleted cell lines were generated in the Flp-In T-Rex HeLa cells [41]. *CEP215* was deleted using CRISPR/Cas9 in *TP53*-deleted cells. The guide RNA (gRNA) sequences for *CEP215* deletion were (5′;-CTGCAGCCGCTGAGCGTCCCAGG −3′;). The triple KO cell was generated in the *PCNT;TP53* double-deleted cells expressing DD-PCNT [41]. The gRNA sequences for CEP215 deletion were (5′;-CCAGGGACGGTGACGTCCTCTTC-3′;) and (5′;-CTGCAGCCGCTGAGCGTCCCAGG-3′;).
For mitotic synchronization, the cells were sequentially treated with 2 mM thymidine (T9250; Sigma-Aldrich, St. Louis, USA) and 5 μM STLC (2191; Tocris Bioscience, Bristol, UK). For the time-course experiment, the cells were treated with doxycycline for 24 h after seeding to induce ectopic expression of PLK4. They were then washed out and cultured for another 24 h. Mitotic cells were obtained with a gentle shake-off from asynchronous cell plates and cultured up to the indicated time points.

Microscopy for live imaging

The coherent anti-stokes raman 167 scattering microscope (TCS SP8 CARS microscope, Leica Microsystems, Wetzlar, Germany) with a 100X objective was used for the live observation of *CETN2-Dendra2* cells. The *CETN2-Dendra2* plasmid [50] was stably transfected into the cells. Then, the cells were synchronized at the M phase with sequential treatments of thymidine (T9250; Sigma-Aldrich, St. Louis, USA) and STLC, activated at 405 nm wavelength for 3 min, and captured at wavelengths of 488 nm and 561 nm for up to 2 h. For the live and immunostaining observation of cells, confocal laser scanning microscope (LSM 700–2, Carl Zeiss, Baden-Wurtte, Germany) was used. The cells were synchronized at the end of G2 phase with sequential treatments of thymidine and RO3306, activated at 405 nm wavelength for 3 min, and released for 30 min. The mitotic cells were shaken off from the plate and moved to a 96-well glass-bottom plates (655090; Greiner Bio-One, Kremsmunster, Austria), stabilized for 2 h, and captured at 488 nm and 561 nm wavelengths. The same cells were fixed and coimmunostained with CETN2 and CEP152.

Microtubule regrowth assay

Mitotic cells were obtained via mitotic shake-off and cultured for 2 h to reach the early G1 phase. The cells were treated with 5 μM nocodazole (M1404; Sigma-Aldrich, St. Louis, USA) at 37°C for 2 h, placed on ice for 1 h, and then transferred to a fresh medium for microtubule growth. The cells were fixed with PEM buffer [80 mM 1,4-Piperazinediethanesulfonic acid (PIPES) pH 6.9, 1 mM magnesium chloride (MgCl2), 5 mM ethyleneglycol-bis (beta-aminoethylether)-N, N'-tetraacetic acid (EGTA), and 0.5% Triton X-100)]

at room temperature for 10 min, incubated in phosphate-buffered saline with 0.5% Triton (PBST) for 5 min to increase permeability, and subjected to immunostaining with antibodies specific to α-tubulin and centrin-2.

Antibodies

Antibodies specific to CETN2 (ICC 1:1000; 04–1624; Merck Millipore, Billerica, MA), CEP295 (ICC 1:500; 122490; Abcam, Cambridge, MA), CEP192 (ICC 1:1000, IB 1:500; A302-324A; Bethyl Laboratories, Montgomery, TX), CEP152 (ICC 1:500, IB 1:100; 183911; Abcam), GAPDH (IB 1: 20000; AM4300; Life Technologies, Carlsbad, CA), SAS6 (ICC 1:200, IB 1:100; sc-376836; Santa Cruz Biotechnology, Dallas, TX, USA), α-tubulin (ICC 1:2000, IB 1: 20000; ab18251; Abcam, Cambridge, MA), γ-tubulin (ICC 1:1000, IB 1:2000; 11316; Abcam, Cambridge, MA), and PARP-1 (IB 1: 1000; 9542; Cell Signaling Technology, Danvers, USA) were purchased. Antibodies specific to CEP215 [55] (ICC 1:2000, IB 1:500), PCNT [60] (ICC 1:2000, IB 1:2000), CEP135 [61] (ICC 1:2000), and CPAP [62] (ICC 1:100; IB 1:500) have been previously described. Secondary antibodies conjugated with fluorescent dyes (ICC 1:1000; Alexa Fluor 488, 594, and 647; Life Technologies) and horseradish peroxidase (IB 1:10000; Sigma-Aldrich, St. Louis, USA) were purchased.

Immunostaining analysis

Cells on a cover glass (0117520; Paul Marienfeld, Lauda-Königshofen, Germany) were fixed with cold methanol for 10 min, washed with cold PBS, and blocked with blocking solution (3% bovine serum albumin and 0.3% Triton X-100 in PBS) for 30 min. The samples were incubated with primary antibodies for 1 h, washed with 0.1% PBST, incubated with secondary antibodies for 30 min, washed, and treated with 4,6-diamidino-2-phenylindole (DAPI) (D9542-5 MG; Sigma-Aldrich, St. Louis, USA) solution for up to 2 min. The cover glasses were mounted on a glass slide with ProLong Gold Antifade Reagent (P36930; Life Technologies, Carlsbad, USA). Images were observed using a fluorescence microscope with a digital camera (Olympus IX51, Olympus, Tokyo, Japan) equipped with QImaging QICAM Fast 1394 and processed in ImagePro 5.0 (Media Cybernetics, Rockville, USA). ImagePro 5.0 (Media Cybernetics, Rockville, USA), Photoshop CC (Adobe, California, USA), and ImageJ 1.51k (National Institutes of Health, Maryland, USA) were used for image processing. All images were obtained in an identical setting with the same exposure time to measure the fluorescence intensities at the centrosome. ImageJ was used for measurement and the background signals were subtracted from the centrosome signals.

Immunoblotting analysis

Cells were washed with PBS, lysed on ice for 10 min with radioimmune precipitation (RIPA) buffer [1% Triton X-100, 150 mM sodium chloride (NaCl), 0.5% sodium deoxycholate, 0.1% sodium dodecyl sulfate (SDS), 50 mM Tris-HCl at pH 8.0, 1 mM sodium orthovanadate (Na3VO4), 10 mM sodium fluoride (NaF), 1 mM ethylenediaminetetraacetic acid (EDTA), and 1 mM EGTA] containing a protease inhibitor cocktail (P8340; Sigma-Aldrich, St. Louis, USA), and centrifuged at 4°C for 10 min. A fraction of the supernatant was used for the Bradford assays and the rest was mixed with 4× SDS sample buffer (250 mM Tris-HCl at pH 6.8, 8% SDS, 40% glycerol, and 0.04% bromophenol blue) and 10 mM dithiothreitol (DTT) (0281–25 G; Amresco, Ohio, USA). The mixture was then boiled for 5 min. For PCNT, CEP215, and CEP152, 3% stacking gel and 4% separating gel were used with 20 mg of each of the protein samples. For SAS6 and CPAP, 5% stacking gel and 8% separating gel were used with 20 mg of each of the protein samples. The remaining samples were loaded in a 5% stacking gel and 10% separating gel with 10 mg of protein samples. Proteins in the gels were then transferred to Protran BA85 nitrocellulose membranes (10401196; GE Healthcare, Chicago, USA). The membranes were blocked with a blocking solution (5% nonfat milk in 0.1% Tween 20 in TBS or 5% bovine serum albumin in 0.1% Tween 20 in TBS) for 2 h, incubated with primary antibodies, diluted in blocking solution overnight at 4°C, washed with TBST (0.1% Tween 20 in TBS), incubated with secondary

antibodies in blocking solution for 30 min, and washed again. Enhanced chemiluminescence (ECL) reagent (LF-QC0101; ABfrontier, Seoul, Korea) and X-ray films (CP-BU NEW; Agfa, Mortsel, Belgium) were used to detect the signals.

Acknowledgments

We thank Professor Alwin Kramer (German Cancer Research Center, Heidelberg, Germany) for providing us with the *pCETN2-Dendra2* plasmid.

Disclosure statement

The authors declare no competing or financial interests.

Funding

This work was supported by the National Research Foundation of Korea (NRF) grant funded by the Korea government [No. NRF-2019R1A2C2002726].

References

[1] Cabral G, Sans S, Cowan C, et al. Multiple mechanisms contribute to centriole separation in C. elegans. Curr Biol. 2013;23(14):1380–1387.
[2] Shukla A, Kong D, Sharma M, et al. Plk1 relieves centriole block to reduplication by promoting daughter centriole maturation. Nat Commun. 2015;6:8077.
[3] Seo M, Jang W, Rhee K. Integrity of the pericentriolar material is essential for maintaining centriole association during M phase. PLoS One. 2015;10(9):e0138905.
[4] Lee K, Rhee K. Separase-dependent cleavage of pericentrin B is necessary and sufficient for centriole disengagement during mitosis. Cell Cycle. 2012;11 (13):2476–2485.
[5] Matsuo K, Ohsumi K, Iwabuchi M, et al. Kendrin is a novel substrate for separase involved in the licensing of centriole duplication. Curr Biol. 2012;22 (10):915–921.
[6] Kim J, Lee K, Rhee K. PLK1 regulation of PCNT cleavage ensures fidelity of centriole separation during mitotic exit. Nat Commun. 2015;6:10076.
[7] Wang W, Soni R, Uryu K, et al. The conversion of centrioles to centrosomes: essential coupling of duplication with segregation. J Cell Biol. 2011;193 (4):727–739.
[8] Novak Z, Gonduit P, Wainman A, et al. Asterless licenses daughter centrioles to duplicate for the first time in Drosophila embryos. Curr Biol. 2014;24 (11):1276–1282.
[9] Fu J, Glover D. How the newborn centriole becomes a mother. Cell Cycle. 2016;15(12):1521–1522.
[10] Tsuchiya Y, Yoshiba S, Gupta A, et al. Cep295 is a conserved scaffold protein required for generation of a bona fide mother centriole. Nat Commun. 2016;7:12567.
[11] O'Connell K, Caron C, Kopish K, et al. The C. elegans zyg-1 gene encodes a regulator of centrosome duplication with distinct maternal and paternal roles in the embryo. Cell. 2001;105(4):547–558.
[12] Bettencourt-Dias M, Rodrigues-Martins A, Carpenter L, et al. SAK/PLK4 is required for centriole duplication and flagella development. Curr Biol. 2005;15(24):2199–2207.
[13] Habedanck R, Stierhof Y, Wilkinson C, et al. The Polo kinase Plk4 functions in centriole duplication. Nat Cell Biol. 2005;7(11):1140–1146.
[14] Ohta M, Tomoko A, Nozaki Y, et al. Direct interaction of Plk4 with STIL ensures formation of a single procentriole per parental centriole. Nat Commun. 2014;5:5267.
[15] Dzhindzhev N, Tzolovsky G, Lipinszki Z, et al. Plk4 phosphorylates Ana2 to trigger Sas6 recruitment and procentriole formation. Curr Biol. 2014;24 (21):2526–2532.
[16] Moyer T, Clutario K, Lambrus B, et al. Binding of STIL to Plk4 activates kinase activity to promote centriole assembly. J Cell Biol. 2015;209(6):863–878.
[17] Lopes C, Jana S, Cunha-Ferreira I, et al. PLK4 trans-autoactivation controls centriole biogenesis in space. Dev Cell. 2015;35(2):222–235.
[18] Arquint C, Gabryjonczyk A, Imseng S, et al. STIL binding to Polo-box 3 of PLK4 regulates centriole duplication. Elife. 2015;4. DOI:10.7554/eLife.07888
[19] Wong C, Stearns T. Centrosome number is controlled by a centrosome-intrinsic block to reduplication. Nat Cell Biol. 2003;5(6):539–544.
[20] Kim M, O'Rourke B, Soni R, et al. Promotion and suppression of centriole duplication are catalytically coupled through PLK4 to ensure centriole homeostasis. Cell Rep. 2016;16(5):1195–1203.
[21] Chan J. A clinical overview of centrosome amplification in human cancers. Int J Biol Sci. 2011;7 (8):1122–1144.
[22] Marteil G, Guerrero A, Vieira A, et al. Over-elongation of centrioles in cancer promotes centriole amplification and chromosome missegregation. Nat Commun. 2018;9(1):1258.
[23] Holland A, Cleveland D. Boveri revisited: chromosomal instability, aneuploidy and tumorigenesis. Nat Rev Mol Cell Biol. 2009;10(7):478–487.
[24] Kleylein-Sohn J, Westendorf J, Clech M, et al. Plk4-induced centriole biogenesis in human cells. Dev Cell. 2007;13(2):190–202.
[25] McCoy R, Demko Z, Ryan A, et al. Common variants spanning PLK4 are associated with mitotic-origin aneuploidy in human embryos. Science. 2015;348 (6231):235–238.

[26] Liao Z, Zhang H, Fan P, et al. High PLK4 expression promotes tumor progression and induces epithelialmesenchymal transition by regulating the Wnt/betacatenin signaling pathway in colorectal cancer. Int J Oncol. 2019;54(2):479–490.
[27] Kong D, Farmer V, Shukla A, et al. Centriole maturation requires regulated Plk1 activity during two consecutive cell cycles. J Cell Biol. 2014;206(7):855–865.
[28] Kong D, Sahabandu N, Sullenberger C, et al. Prolonged mitosis results in structurally aberrant and over-elongated centrioles. J Cell Biol. 2020;219:6.
[29] Kohlmaier G, Loncarek J, Meng X, et al. Overly long centrioles and defective cell division upon excess of the SAS-4-related protein CPAP. Curr Biol. 2009;19 (12):1012–1018.
[30] Fu J, Glover D. Structured illumination of the interface between centriole and peri-centriolar material. Open Biol. 2012;2(8):120104.
[31] Lawo S, Hasegan M, Gupta G, et al. Subdiffraction imaging of centrosomes reveals higher-order organizational features of pericentriolar material. Nat Cell Biol. 2012;14(11):1148–1158.
[32] Mennella V, Keszthelyi B, McDonald K, et al. Subdiffraction-resolution fluorescence microscopy reveals a domain of the centrosome critical for pericentriolar material organization. Nat Cell Biol. 2012;14 (11):1159–1168.
[33] Doxsey S, Stein P, Evans L, et al. Pericentrin, a highly conserved centrosome protein involved in microtubule organization. Cell. 1994;76(4):639–650.
[34] Andersen J, Wilkinson C, Mayor T, et al. Proteomic characterization of the human centrosome by protein correlation profiling. Nature. 2003;426(6966):570–574.
[35] Fong K, Choi Y, Rattner J, et al. CDK5RAP2 is a pericentriolar protein that functions in centrosomal attachment of the gamma-tubulin ring complex. Mol Biol Cell. 2008;19(1):115–125.
[36] Dictenberg J, Zimmerman W, Sparks C, et al. Pericentrin and gamma-tubulin form a protein complex and are organized into a novel lattice at the centrosome. J Cell Biol. 1998;141(1):163–174.
[37] Kim S, Rhee K. Importance of the CEP215-pericentrin interaction for centrosome maturation during mitosis. PLoS One. 2014;9(1):e87016.
[38] Bond J, Roberts E, Springell K, et al. A centrosomal mechanism involving CDK5RAP2 and CENPJ controls brain size. Nat Genet. 2005;37(4):353–355.
[39] Rauch A, Thiel C, Schindler D, et al. Mutations in the pericentrin (PCNT) gene cause primordial dwarfism. Science. 2008;319(5864):816–819.
[40] Delaval B, Doxsey S. Pericentrin in cellular function and disease. J Cell Biol. 2010;188(2):181–190.
[41] Kim J, Kim J, Rhee K. PCNT is critical for the association and conversion of centrioles to centrosomes during mitosis. J Cell Sci. 2019;132:6.
[42] Srsen V, Gnadt N, Dammermann A, et al. Inhibition of centrosome protein assembly leads to p53-dependent exit from the cell cycle. J Cell Biol. 2006;174 (5):625–630.
[43] Lambrus B, Uetake Y, Clutario K, et al. p53 protects against genome instability following centriole duplication failure. J Cell Biol. 2015;210(1):63–77.
[44] Barrera J, Kao L, Hammer R, et al. CDK5RAP2 regulates centriole engagement and cohesion in mice. Dev Cell. 2010;18(6):913–926.
[45] Pagan J, Marzio A, Jones M, et al. Degradation of Cep68 and PCNT cleavage mediate Cep215 removal from the PCM to allow centriole separation, disengagement and licensing. Nat Cell Biol. 2015;17(1):31–43.
[46] Citron Y, Fagerstrom C, Keszthelyi B, et al. The centrosomin CM2 domain is a multi-functional binding domain with distinct cell cycle roles. PLoS One. 2018;13(1):e0190530.
[47] Gillingham A, Munro S. The PACT domain, a conserved centrosomal targeting motif in the coiled-coil proteins AKAP450 and pericentrin. EMBO Rep. 2000;1(6):524–529.
[48] Coelho P, Bury L, Shahbazi M, et al. Over-expression of Plk4 induces centrosome amplification, loss of primary cilia and associated tissue hyperplasia in the mouse. Open Biol. 2015;5(12):150209.
[49] Wong Y, Anzola J, Davis R, et al. Cell biology. reversible centriole depletion with an inhibitor of polo-like kinase 4. Science. 2015;348(6239):1155–1160.
[50] Loffler H, Fechter A, Liu F, et al. DNA damage-induced centrosome amplification occurs via excessive formation of centriolar satellites. Oncogene. 2013;32(24):2963–2972.
[51] Hatch E, Kulukian A, Holland A, et al. Cep152 interacts with Plk4 and is required for centriole duplication. J Cell Biol. 2010;191(4):721–729.
[52] Cizmecioglu O, Arnold M, Bahtz R, et al. Cep152 acts as a scaffold for recruitment of Plk4 and CPAP to the centrosome. J Cell Biol. 2010;191(4):731–739.
[53] Izquierdo D, Wang W, Uryu K, et al. Stabilization of cartwheel-less centrioles for duplication requires CEP295-mediated centriole-to-centrosome conversion. Cell Rep. 2014;8(4):957–965.
[54] Watanabe K, Takao D, Ito K, et al. The Cep57-pericentrin module organizes PCM expansion and centriole engagement. Nat Commun. 2019;10(1):931.
[55] Lee S, Rhee K. CEP215 is involved in the dynein-dependent accumulation of pericentriolar matrix proteins for spindle pole formation. Cell Cycle. 2010;9(4):774–783.
[56] Barr A, Kilmartin J, Gergely F. CDK5RAP2 functions in centrosome to spindle pole attachment and DNA damage response. J Cell Biol. 2010;189(1):23–39.
[57] Kim T, Park J, Shukla A, et al. Hierarchical recruitment of Plk4 and regulation of centriole biogenesis by two centrosomal scaffolds, Cep192 and Cep152. Proc Natl Acad Sci U S A. 2013;110(50):E4849–57.
[58] Chinen T, Yamazaki K, Hashimoto K, et al. Centriole and PCM cooperatively recruit CEP192 to spindle

poles to promote bipolar spindle assembly. J Cell Biol. 2021;220(2). DOI:10.1083/jcb.202006085

[59] Ganem N, Godinho S, Pellman D. A mechanism linking extra centrosomes to chromosomal instability. Nature. 2009;460(7252):278–282.

[60] Lee K, Rhee K. PLK1 phosphorylation of pericentrin initiates centrosome maturation at the onset of mitosis. J Cell Biol. 2011;195(7):1093–1101.

[61] Kim K, Lee S, Chang J, et al. A novel function of CEP135 as a platform protein of C-NAP1 for its centriolar localization. Exp Cell Res. 2008;314 (20):3692–3700.

[62] Chang J, Cizmecioglu O, Hoffmann I, et al. PLK2 phosphorylation is critical for CPAP function in procentriole formation during the centrosome cycle. EMBO J. 2010;29(14):2395–2406.